JOURNAL OF MATERIALS SCIENCE 4 (1969) 499–508

Solution Hardening of Lead Single Crystals at Liquid Air Temperature

J. VAN DER PLANKEN, A. DERUYTTERE
Instituut voor Metaalkunde, Katholieke Universiteit, Leuven, Belgium

Recieved 11 December 1968

Single crystals of lead with either thallium, indium, bismuth, cadmium, mercury or antimony were tested in tension in liquid air. The critical resolved shear stress τ_0 increases linearly with increasing solute content c in a limited concentration range. The increase $\Delta\tau_0/\Delta c$ is lowest for lead-thallium and highest for lead-antimony. When log $\Delta\tau_0/\Delta c$ is plotted against log (sf + elf) where sf $= [(d_1)_{Pb} - (d_1)_{sol}/(d_1)_{Pb}]10^2$, d_1 being the closest distance of approach, and elf $= \Sigma$En, ΣEn being the sum of the electronegativities of solvent and solute, a straight line of slope 2 results. A similar result is obtained with data from the literature for single crystals of copper alloys and of magnesium alloys. However in these cases a different size factor has to be used.

1. Introduction

Haasen [1] has given a detailed survey of the theories about solution-hardening, mainly in fcc metals. The experimental investigations have been adequately summarised by Hibbard [2] and Haasen [1]. Some experimental results agree with existing theories, others do not. Thus Linde and Edwardson [3] plotted the increase of critical resolved shear stress (crss) per at. % solute of binary copper single crystals, pulled at room temperature against a size factor, and found a quadratic relationship as proposed in the original Mott–Nabarro theory [4]. However the results for Cu–Si and Cu–Ni alloys did not fit. Moreover the absolute values of the crss, computed from the Mott and Nabarro formula, were too small by two orders of magnitude. The later modification of this theory [5] gave a rather good agreement with some of the absolute experimental values of Linde and Edwardson, but the power 4/3 for the size factor was not in accordance with the experimental data.

Fleischer [6-8] determined the concentration dependence of the yield stress of polycrystalline binary copper alloys. He found that on the average 75% of the total hardening is due to a modulus effect and only 25% to a size effect. Fleischer reached two other conclusions: (i) the yield stress variation of copper alloys is mainly due to the interaction of screw dislocations with the solute atoms; (ii) the effect of valency differences between solute and solvent is sufficiently accounted for by the elastic modulus term.

The theory of Fleischer can be criticised because only the interactions between dislocations and the closest solute atoms are considered. Later it was found that Fleischer's analysis does not work for polycrystalline binary niobium alloys [9]: the modulus effect contributes, but is not the main factor. Apparently the assumptions made by Fleischer are not entirely valid for a highly anisotropic structure such as that of niobium.

In recent work on the solute-hardening in polycrystalline silver base alloys [10], Hutchison and Honeycombe found considerable scatter when plotting the yield stress increase against the parameter of the Fleischer model. Yet Fleischer had found good agreement with this theory for the hardness increments of polycrystalline silver alloys against the same parameter. Hutchison and Honeycombe noted however that the apparently good correlation found by Fleischer decreased markedly when other published values of the shear modulus variation were used. These authors describe solution-hardening of silver alloys in terms of temperature-dependent and temperature-independent components [1], both of which are related to the electronic influence of the solute.

Hitherto, very few experiments have concerned the solution-hardening in polyvalent fcc metals. An early investigation by Goebel [11] deals with the increase in hardness of polycrystalline lead alloyed with antimony, arsenic, bismuth, cadmium, magnesium, mercury, sodium and tin. The tensile properties of aluminium solid solutions in relation to changes in lattice parameter led Dorn, Pietrowsky and Tietz [12] to the conclusion that solution hardening is intimately related to metallic bonding. However to explain their results, Dorn *et al* attributed a valency of two to aluminium. Hardie and Parkins [13] plotted the change in lattice parameter of binary aluminium alloys against the hardness increment due to the addition of 1 at. % solute. A straight line was obtained, but Al–Mg and Al–Ag alloys did not fit. These authors suggested that the hardening of aluminium by silver, that of copper by silicon and of lead by sodium is due to chemical affinity effects in the absence of lattice distortion.

In the present work the hardening at liquid air temperature of lead single crystals by the addition of thallium, indium, cadmium, mercury and antimony was studied by means of tensile tests.

2. Experimental Procedure

2.1. Single Crystal Preparation

Because of the importance of purity in research on single crystals, particularly in the case of lead [14, 15], a list of the purity of the metals used in this work is given in table I. Lead of two grades was used for the tests on pure lead. The alloys were prepared only with the purest lead. The metals were melted, thoroughly mixed and poured into a preheated split steel mould (5 mm diameter by 250 mm length). In order to prevent sticking of the rods to the walls, the mould was coated with graphite. The best rods were always obtained in a mould preheated just above the melting point. The rods were cleaned and enclosed in evacuated precision bore pyrex tubes, which had been internally coated with graphite. Single crystals were prepared by a modified Bridgman technique at speeds of 5 cm/h and a temperature gradient of 17° C/cm, except for Pb–Cd for which the conditions were 2 cm/h and 25° C/cm.

The percentage of solute added was limited to 1 at. % for Bi, Cd and Sb, and to 2 at. % for Hg. Pb–In single crystals could be prepared up to 20 at. % and Pb–Tl up to 65 at. %. The single crystals were carefully withdrawn from the tube and etched in the solution given by Fleischer [14] for lead, which was satisfactory for most alloy compositions. A Laue back reflection photograph was used to determine the orientation. The spots revealed some substructure in all cases even for the high purity lead. A homogenising treatment was not applied.

2.2. Test Procedure

The crystals were flame- or acid-cut into lengths of nearly 7 cm and mounted in conical copper grips: their ends were then arc-melted to form shoulders in the grips. In that way a gauge length of 5 cm was obtained. The copper grips were attached to the chucks of a Hounsfield Tensometer by means of thin wires. The single crystals, immersed in liquid air, were deformed to rupture at constant crosshead speed (initial elongation rate 1.7×10^{-3} sec^{-1}). The load/elongation diagram was hand recorded and converted into shear stress/shear strain curves supposing $\{1\,1\,1\}\langle\bar{1}\,0\,1\rangle$ slip. The symbols used for the characteristic parameters of these curves are those used for instance by Seeger *et al* [16].

After each test the two extremities of the crystal were used for chemical analysis.

3. Experimental Results

3.1. Pure Lead

The shear stress/shear strain curves exhibit the classical three stages of fcc single crystals (fig. 1) for the 99.98% and 99.999% lead. The mean values of the crss for these two purity grades differ by about 6% (table II). An interesting feature is that the crss of specimens cut from the same crystal decreases with increasing distance from the first solidified end (table III). This may indicate that contamination occurred during preparation of the alloy with subsequent segregation during single crystal growth. In table IV the present results and test conditions are compared with those from the literature.

Feltham and Meakin [17] made their tensile tests on a tensometer similar to ours. They failed

TABLE I Purity of the metals used.

Metal	Pb	Pb	In	Bi	Sb	Tl	Cd	Hg
Purity %	99.98	> 99.999	> 99.999	> 99.999	> 99.99	> 99.999	> 99.99	99.9

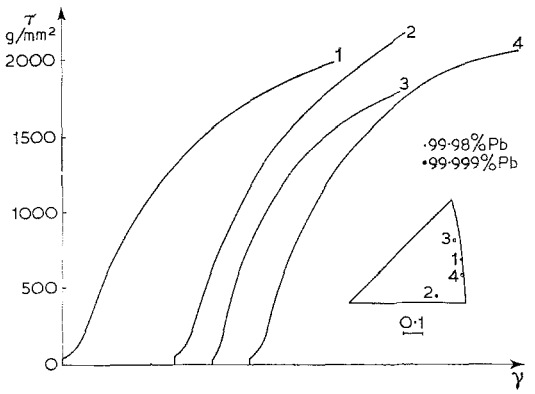

Figure 1 Shear stress/shear strain curves and orientation of lead crystals of two purities.

TABLE II crss of lead of two purity grades at 78° K.

τ_0 g/mm²	Number of tests	Purity %
53.7	5	99.98
50.6	9	> 99.999

TABLE III crss of three specimens cut from the same crystal.

	τ_0 g/mm²
First solidified end	53.1
Middle part	47.5
Last solidified end	44.7

to find an easy glide region and their crss value is high. Fleischer [14] undertook a special investigation on the anomalous absence of easy glide and considered three possible factors, viz. crystal dimensions, temperature and purity. He attributed the anomaly to the presence of certain impurities in the lead used. He apparently overlooked another factor which may be of decisive influence, viz. the treatment of the crystal prior to the test. The single crystals used by Feltham and Meakin had a cross-section of only about 7 mm², which corresponds, for a crss of 50 g/mm², to a tensile load of approximately 700 g. Such crystals should easily become bent on mounting. Weinberg [15] found three different values depending on the treatment of the lead single crystals between growth and testing. He found that the crss is decreased by annealing before mounting on the tensile machine. If the anneal was done *in situ* after mounting, the crss, and also the scatter, was further reduced. These data are given in table IV.

In the present investigation the handling and mounting were done with utmost care, and the crystals of 99.98 % purity, i.e. less pure than those used by Feltham and Meakin, did show an easy glide region much the same as in the crystals of 99.999 % purity. The shear stress/shear strain curves show the same characteristics as for other fcc metals: towards the corners of the stereographic triangle, the work hardening rate θ_I in the easy glide stage and the shear stress τ_{II} at the intersection of part I and part II, increase. The same conclusion had been reached by Bolling, Hays and Wiedersich [18]. The extent of the easy glide region is limited ($\gamma_{II} = 0.034$ to 0.080) but much larger than that found by the above mentioned authors. The τ_{II}/τ_0 (τ_{II} shear stress at the intersection of the easy glide region and the second stage, τ_0 critical resolved shear stress) ratio ranges from 1.55 to 1.95 with an overall average of 1.74, in good agreement with the value of 1.75 found by Bolling *et al*, whereas Fleischer found 1.68. In the linear hardening stage the work-hardening rate θ_{II} ranges from 3.3 to 5 $\times$ 10^{-3}G (G shear modulus of lead at liquid air temperature). The shear stress τ_{III} at the end of this region is difficult to determine accurately because of the very smooth transition to the third stage. It varies from 609 to 645 g/mm².

TABLE IV Summary of the crss of lead at 78° K from literature.

Authors	τ_0 g/mm²	Purity %	Strain rate sec^{-1}	Dimensions mm	Ref.
P. Feltham, J. D. Meakin	127	> 99.99	1×10^{-4}	$3^{\phi} \times 50$	17
P. W. Neurath, J. S. Koehler	96 ± 8	> 99.999	*	$5^{\phi} \times 50$	19
G. F. Bolling, L. E. Hays, H. W. Wiedersich	55	Zone ref.	0.0016 to 15.4 $\times$ 10^{-3}	$8^{\phi} \times 50$	18
R. L. Fleischer	44	> 99.999	0.4 and 0.8 $\times$ 10^{-4}	4.4 × 6.6 × 40	14
F. Weinberg as-grown	72	99.999	1.7×10^{-4}	6.5 × 3.3 × 50	15
annealed	43.6	and			
annealed *in situ*	34	99.9999			
Present results	53.7	99.98	1.7×10^{-3}	$5^{\phi} \times 50$	
	50.6	99.999	1.7×10^{-3}	$5^{\phi} \times 50$	

*Creep tests.

TABLE V Comparison of the weakly orientation dependent parameters of the τ, γ curves of lead at 78° K.

Authors	τ_0 g/mm²	θ_{II} 10^3G	τ_{III} g/mm²	τ_{II} g/mm²	τ_{II}/τ_0	Ref.
P. Feltham, J. D. Meakin	127	2.1	*	*	*	17
G. F. Bolling *et al*	55	2.9	667.3	87.2	1.75	18
R. L. Fleischer	44	4.3	*	73.3	1.68	14
Present work	53.7 (99.98)	3.3	609	86.9	1.67	
	50.6 (99.999)	5	645	79.7	1.74	

*Not given.

Table V compares some parameters of the shear stress/shear strain curves of lead at 78° K.

3.2. Lead-Indium

Lead dissolves about 70 at. % indium but the liquidus and solidus curves separate more and more with increasing solute content. This was probably the reason why repeated attempts to produce good single crystals having an indium content higher than 20 at. % failed.

Single crystals containing 0.2, 0.4, 0.8, 5, 10 and 20 at. % indium were easily obtained, but the Laue spots of the 20 at. % alloys were markedly split. Fig. 2 shows some of the shear stress/shear strain curves of crystals having similar orientations. The crss increases linearly

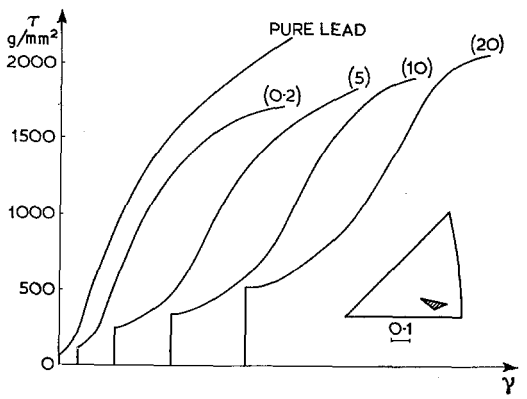

Figure 2 Shear stress/shear strain curves and orientation of lead and lead-indium of comparable orientation. The figures between brackets indicate the indium co ıtent (at. %).

with increasing indium content [fig. 3] up to 10 at. % indium. The intersection with the ordinate axis nearly coincides with the experimentally determined value for pure lead (see table II). Table VI gives the constants of the equation $\tau_0 = Ac + B$ for the Pb–In system and also for the systems discussed below.

The shear stress/shear strain curves show the following special features:

(i) There are two linear portions in the easy glide region for crystals containing at least 5 at. % solute; the hardening rate in the first portion is very low (fig. 2).

(ii) After unloading the specimen in the easy glide or in the linear hardening stage the slight sloping region appeared again on reloading. During this operation the crystal remained in the liquid air bath.

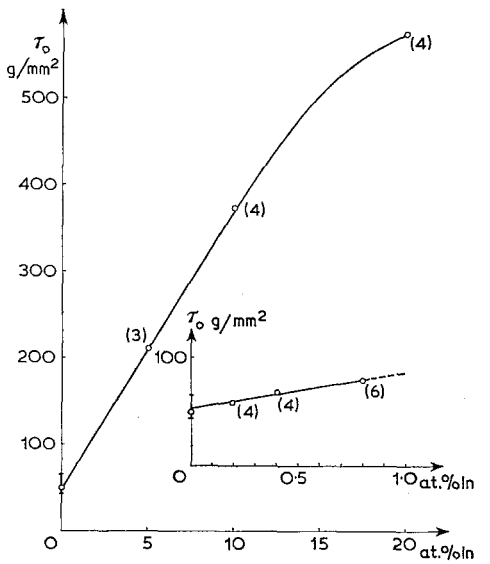

Figure 3 Increase of crss plotted against at. % indium. The figures between brackets give the number of tests.

TABLE VI Values of the constants of the equation $\tau_0 = Ac + B$ and concentration interval in which the relation holds.

Solute	A g/mm² at. %	B g/mm²	Interval at. %	Ref.
Tl	10.1	30.2	2 to 15	
In	31.9	51.5	0 to 12	
Bi	57.0	59.1	0 to 1	
Sn	70.0	32.0	0 to 0.4	Fleischer [14]
Cd	102.2	52.1	0 to 1	
Hg	135.2	49.2	0 to 2	
Sb	74.0	48.8	0 to 0.2	
	189.1	21.0	0.2 to 0.5	

3.3 Lead-Thallium

Lead dissolves thallium to a high concentration (~ 87 at. %) and the distance between liquidus and solidus curves is negligibly small up to 62.5 at. % thallium, at which composition a maximum occurs.

Single crystals have been prepared containing nominally 2, 6, 15, 30, 50 and 65 at. % thallium. Only with the 65 at. % alloy was the splitting of the Laue spots more pronounced than with pure lead. Fig. 4 gives the orientation and the shear stress/shear strain curves of some of these alloy crystals. They exhibit the same special features as

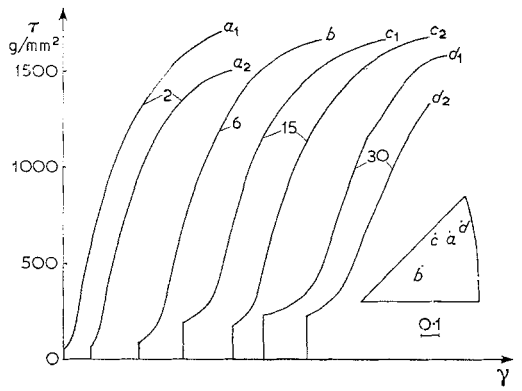

Figure 4 Shear stress/shear strain curves and orientation of lead-thallium alloys. The figures indicate the thallium content (at. %). Note the kink in the curve of crystal d_1.

those of the lead-indium crystals but now at higher solute contents ($\geqslant$ 15 at. %). Up to 2 at. % thallium the crss is not affected. From 2 to 15 at. % the increase is linear (constants of $\tau_0 = Ac + B$ in table VI). If τ_0 is plotted against the square root of the thallium concentration a linear relationship is obtained, covering the whole range up to 65 at. % [fig. 5] $\tau_0 = 48.77 \sqrt{c} - 21$.

The 50 at. % specimens behave completely differently: the load/elongation diagram consists of horizontal parts connected by small upwards jumps and the crystal deforms heterogeneously. This phenomenon will be discussed elsewhere [20]. In one test (crystal d_1 of fig. 4) a kink occurred in the stress/strain curve and the hardening rate was suddenly halved. The shear stress at this point was considered to be τ_{III}. The same feature was frequently observed by Bolling *et al* [18] in pure lead, though the change in slope was smaller than in this case. In the present work it was not observed with pure lead.

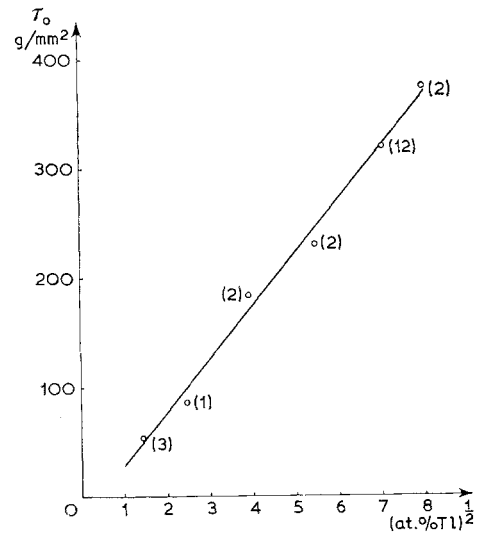

Figure 5 Increase of crss as a function of (at. %)$^{1/2}$ for lead-thallium. The figures between brackets are the number of tests.

3.4. Lead-Antimony

The solubility of antimony in lead diminishes from 5.8 at. % at 252° C to 0.75 at. % at 100° C. A precipitate of Sb is therefore not impossible in the slowly cooled single crystals containing more than 0.75 at. % antimony. Single crystals of 0.14, 0.49 and 0.90 at. % antimony were grown without difficulty. The extent of the easy glide region increases regularly with rising solute content; this is an indication of the absence of a precipitate. The τ_0, c relation is not so simple as for the Pb–In alloys. It is represented in fig. 6 and the constants of the τ_0, c equation are given in table VI.

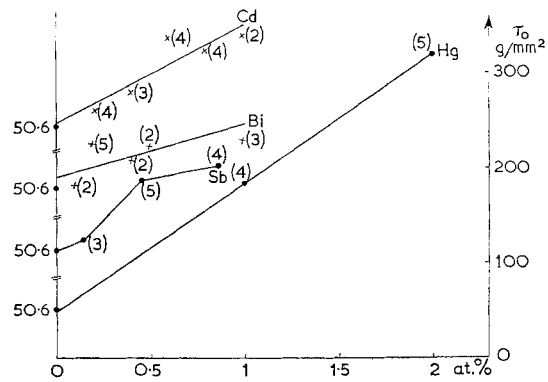

Figure 6 Plot of crss against composition for lead-antimony lead-mercury, lead-cadmium and lead-bismuth alloys. The figures between brackets are the number of tests.

The extrapolation of the line linking the results for the 0.14 and 0.49 crystals gives too low a value for pure lead (21 g/mm²). The straight line connecting the experimental plot of pure lead and the average value for the 0.14 alloys has a much lower slope (table VI).

3.5. Lead-Mercury

Lead dissolves 24 at. % mercury at 140° C as well as at room temperature. Single crystals containing 1 and 2 at. % mercury were easily obtained. However, etching in the same solution as was used for the other alloys and for lead, resulted in a bright polished surface. A series of Laue photographs was taken to check whether the crystals were single. As with lead-thallium and lead-indium the easy glide region shows two distinct linear parts having the same features as in the above mentioned alloys, but occurring at low solute contents. The crss of pure lead increases linearly with the mercury content (fig. 6). Table VI gives the constants of the τ_0, c equation.

3.6 Lead-Cadmium

The solubility of cadmium is 5.9 at. % at the eutectic temperature (248° C) and falls down rapidly with decreasing temperature to 0.7 at. % at 100° C. Therefore Cd could precipitate during single crystal growth. Single crystals were prepared containing 0.2, 0.4, 0.6, 0.8 and 1.0 at. % cadmium at the usual conditions, i.e. 5 cm/h and 17° C/cm. Unlike the other alloys, a well-developed mosaic structure resulted. By changing to 2 cm/h and 25° C/cm the quality of the crystals was much improved. As with lead-mercury the extent of the easy glide region is very sensitive to cadmium additions. The crss increases linearly with cadmium concentration (fig. 6). The τ_0, c relation is characterised by the constants given in table VI. A feature of all the crystals tested was a higher crss for the last solidified part of the single crystal: this tendency was most pronounced in lead-cadmium alloys. However chemical analyses did not reveal any composition difference.

3.7 Lead-Bismuth

Though the solubility of bismuth in lead is 23.3 at. % at the peritectic temperature (184° C), and still 18 at. % at 0° C, many difficulties occurred during the preparation of the single crystals and the interpretation of the results. Etching appeared to be almost impossible and single crystals with more than 1 at. % bismuth were very difficult to obtain.

Laue photographs were used to check whether the specimens were single crystals. The increase of the easy glide region at the concentrations tested is small and the crss was difficult to determine, partly because the orientations were close to the sides of the orientation triangle.

According to Hofmann [21] the recrystallisation rate of lead is increased by the addition of bismuth, at least at room temperature. This may have affected the present results. The constants of the equation representing the least squares straight line in a τ_0, c diagram (fig. 6) are given in table VI.

The extrapolated value for lead is rather high mainly because of the abnormally high result for the 0.2 at. % alloy. However, neglecting this result would not much affect the slope of the line.

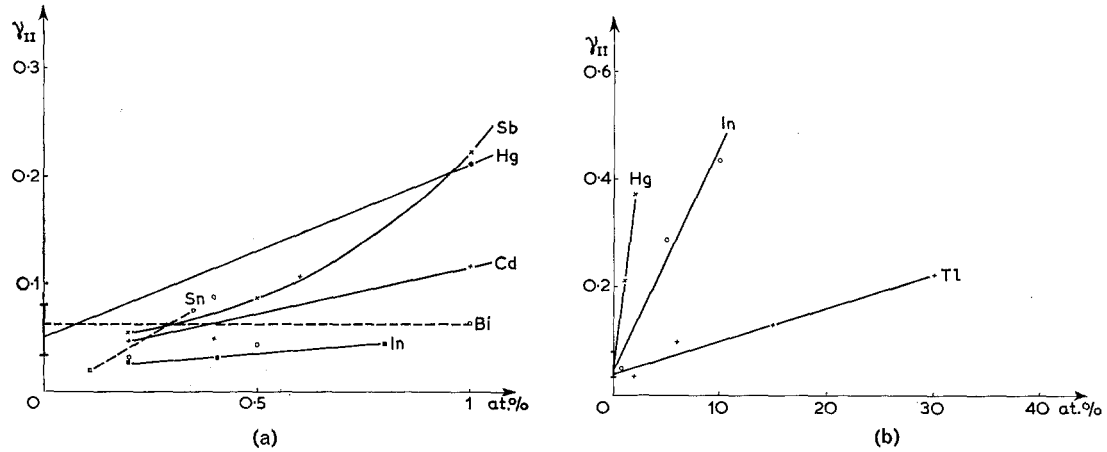

Figure 7(a) Extent of easy glide region of lead (γ_{II}) as a function of solute content for various elements up to 1 at. % addition. (b) Extent of easy glide region of lead (γ_{II}) plotted versus solute content for mercury, indium and thallium.

4. Summary and Discussion

4.1. Variation of the crss with Solute Concentration

The crss of the binary alloys studied as a function of concentration, can be represented by a linear relationship, at least in a limited concentration range. Table VI gives for the different solutes the constants of the straight line equation and the concentration interval in which the measurements were made or in which the relation holds. The results of Fleischer [14] on lead-tin are included.

As previously stated, for the lead-thallium alloys, a better representation with the relation $\tau_0 = C\sqrt{c} + D$ is obtained if the concentration range 0 to 65 at. % is considered.

4.2. The Shear Stress/Shear Strain Curves

Lead belongs to the "intermediate class" of metals together with copper, nickel, gold and silver as regards γ_{st}/Gb [15], where γ_{st} denotes stacking fault energy, and the conclusions of Diehl [22] about the plastic deformation of copper single crystals, appear also to hold here [14]. The situation for the alloys is more complicated. Near to the ⟨100⟩ and ⟨111⟩ axis, or near to the ⟨100⟩ to ⟨111⟩ symmetry line, the easy glide region tends to decrease or disappears completely. However, this behaviour depends on the solute element: in the lead-antimony single crystals the increase of γ_{II} (= extent of easy glide region) is appreciable (fig. 7a), even at the low percentages studied, and the effect of orientation is very small. The same remark holds for lead-mercury and lead-cadmium (fig. 7a, b).

Lead-bismuth on the other hand does not show extensive easy glide regions even with "soft" orientations. With concentrated alloys the orientation dependence of the shear stress/shear strain parameters is greatly reduced. However, the distinction between concentrated and dilute alloys is not so clear cut since 1 % of either antimony, mercury or cadmium can be considered as high concentrations much the same as 5 % indium or 10 % thallium. According to Fleischer [14] the solubility should play an important role. From the present work it appears that this is not the only determining factor, since the solubility of mercury (24 at. %) and bismuth (23.3 at. %) do not differ much, though the influence on the stress/strain curve is very different: bismuth behaves like a nearly insoluble element. The marked contrast between antimony and cadmium (5.8 and 5.9 % solubility) in their influence on the stress/strain curves is another example.

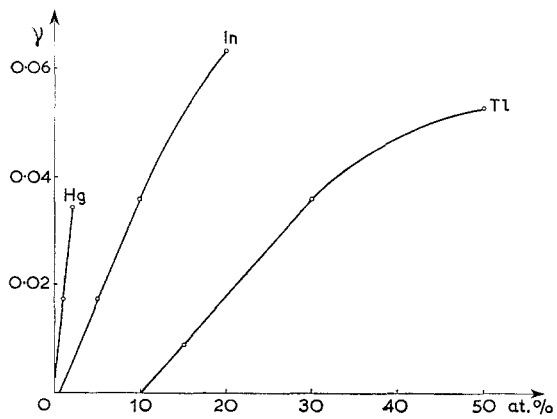

Figure 8 Extent of first linear part of the easy glide region as a function of solute content for mercury, indium and thallium.

As already mentioned, lead-thallium, lead-indium and lead-mercury single crystals exhibit two linear portions in the easy glide region. The extent of the first part increases with increasing solute content (fig. 8). The close resemblance between fig. 7b and fig. 8 is obvious. The work hardening in this part of the curve is 0.2 to 3×10^{-4} G_{Pb} (G_{Pb} shear modulus of lead). In the second stage $G/\theta_{II} = 334$ to 1370 for pure lead. In the alloys studied θ_{II} decreases with increasing solute concentration, except for lead-mercury where the reverse is true. To our knowledge the change of G with composition is not known for lead alloys except for lead-thallium [23]. Specimens from the initially solidified part of the crystals had higher θ_{II} values in the case of lead-indium, lead-thallium and lead-cadmium; for lead-mercury and lead-bismuth the reverse is true; lead-antimony shows no special trend. The results of the chemical analyses did not reveal any concentration gradient along the crystal, and agreed within experimental error with the nominal composition.

4.3. Solution-Hardening of Lead

When the increase of crss per at. % solute is plotted against the size misfit $\Delta a/a\, \Delta c$ [4], a diffuse picture results, both when the lattice parameter variation calculated from published values [24, 25] and when the linear size factor (lsf) of King [26] is used. Although King used the same sources his values differ appreciably from ours for lead-mercury, lead-cadmium and lead-antimony (compare in table VII the values of

TABLE VII Characteristics of binary lead alloys.

Element	$\Delta\tau_0/\Delta c$ g/mm² at. %	$\lvert \Delta a/a\,\Delta c \rvert 10^4$ [24, 25]	| lsf | [26]	Max. sol. (at. %)	En [27]	sf *	ΣEn
Pb					1.56		
Tl	10.1	1.42	11.53	87.5	1.90	2.6	3.46
In	31.9	3.70	3.87	70.0	1.36	7.2	2.92
Bi	57.0	2.43	2.29	23.3	1.59	11.0	3.15
Sn	70.0	2.81	2.83	29.0	1.50	13.6	3.06
Cd	102.2	4.66	17.14	5.9	1.09	14.9	2.65
Hg	135.2	7.21	1.78	24.0	1.09	14.2	2.65
Sb	189.1	1.09	4.93	5.8	2.10	16.9	3.66

* $\left|\frac{(d_1)_{Pb} - (d_1)_{sol}}{(d_1)_{Pb}}\right| 10^2$

$\Delta a/a\,\Delta c$ with those denoted lsf, which should be identical).

A much clearer picture is obtained (fig. 9) if the hardening is plotted against the solid solubility size factor defined as

$$\text{sf} = \left[\frac{(d_1)_{Pb} - (d_1)_{sol}}{(d_1)_{Pb}}\right] \times 10^2$$

where d_1 is the closest distance of approach, and sol refers to solute.

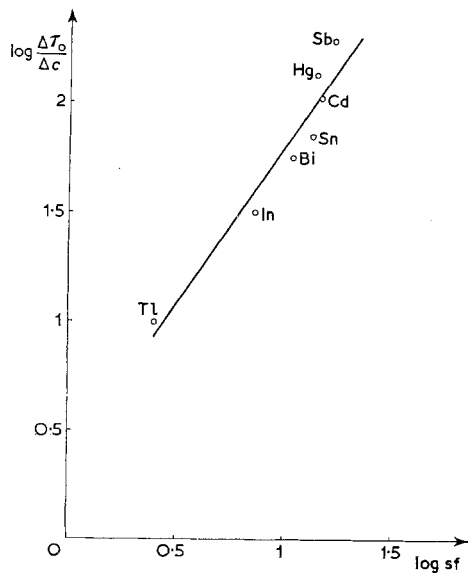

Figure 9 Solution-hardening ($\Delta\tau_0/\Delta c$) of lead plotted versus size factor (sf). The size factor is defined as $\text{sf} = [(d_1)_{Pb} - (d_1)_{sol}/(d_1)_{Pb}]10^2$ where d_1 is closest distance of approach and sol refers to solute.

The hardening increases now with increasing size factor. An attempt was made to reduce the scatter by taking into account electronic effects. Solution hardening should be accounted for by a size factor and an "electronic factor", e.g. according to the equation

$$\frac{\Delta\tau_0}{\Delta c} = k_1\,[(\text{sf}) + k_2(\text{elf})]\,k_3$$

where k_1, k_2 and k_3 are constants, (sf) is the size factor, (elf) the electronic factor. The above equation was put into an IBM ordinator 360 and different data were used for the size-factor and for the electronic factor. The best result was obtained by using the sum of the electronegativities of the two elements concerned, (ΣEn) for (elf) and the above relation for sf [fig. 10]. Introducing the shear modulus of lead the following relationship is obtained:

$$\frac{\Delta\tau_0}{\Delta c} = 0.31 \times G_{Pb} \times 10^{-6}\,[(\text{sf}) + \Sigma\text{En}]^{2.04}$$

The electronegativity data given by Teatum *et al*

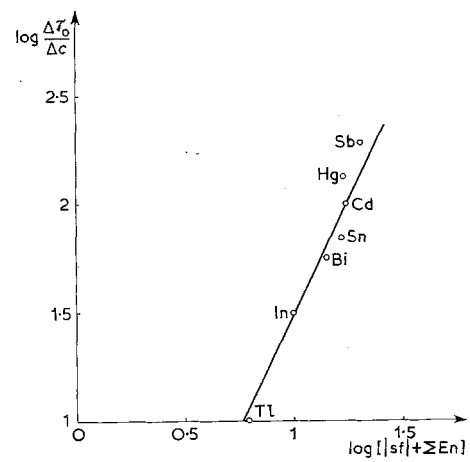

Figure 10 Solution-hardening of lead plotted versus sum of size factor and ΣEn. ΣEn is the sum of the electronegativities of the two elements concerned.

[27] were used. Table VII lists the values of En of the various elements.

When the same procedure is applied to the data for binary copper-base single crystals [3] the following result is obtained (fig. 11):

$$\frac{\Delta\tau_0}{\Delta c} = 0.90 \times G_{Cu} \times 10^{-6}\,[(\text{lsf}) + \Sigma\text{En}]^{1.89}$$

where lsf is the linear size factor as given by King [26]. The results for Cu–Ni and Cu–Si fit well.

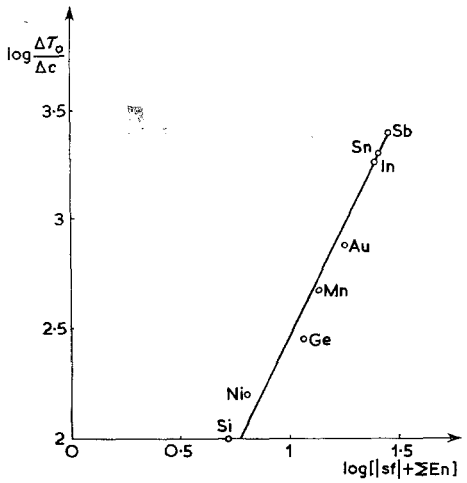

Figure 11 Solution-hardening of copper ($\Delta\tau_0/\Delta c$) plotted versus (lsf) + ∑En where lsf is the linear size factor [26] and ∑En the sum of the electronegativities of the two elements concerned.

Fig. 12 shows a similar plot for magnesium alloy single crystals, fitting the equation:

$$\frac{\Delta\tau_0}{\Delta c} = 0.79 \times G_{Mg} \times 10^{-6}[(\text{sf}) + \Sigma\text{En}]^{1.85}$$

Here the best result is obtained when the size factors of Wilson [29] are used, but the scatter is still appreciable for the lithium and indium alloys. It should be noted that no clear picture resulted when the electronegativity difference was used as in Waber *et al* [28] for the solid solubility.

From the foregoing it appears impossible to define an "all-purpose size factor" that can be used for the three series of alloys. For copper the best correlation is obtained with the lattice parameter variation, for lead with the relative difference in closest distance of approach and for magnesium with the size factor determined by Wilson [29]. A term has to be introduced that

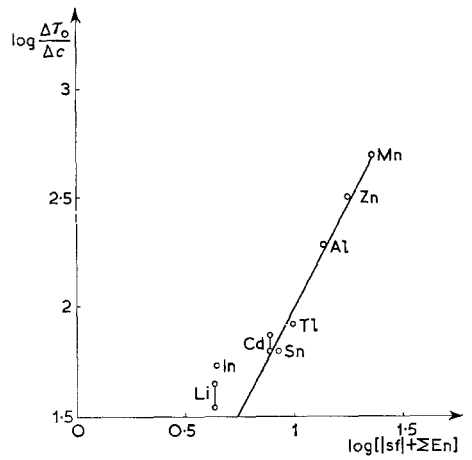

Figure 12 Solution-hardening of magnesium ($\Delta\tau_0/\Delta c$) plotted versus sf + ∑En where sf is the size factor [29] and ∑En the sum of the electronegativities of the two elements concerned.

accounts for electronic effects. The electronegativity is a measure of the attraction of electrons to the atom. For a given size factor the dipole character of edge dislocations will be the more pronounced, the greater ΣEn. Therefore the interaction of dislocations with solute atoms and the hardening should increase with ΣEn. Cottrell, Hunter and Nabarro [30] calculated that the role of the electrical interaction in binary copper alloys is secondary to that of the elastic interaction and amounts to between 1/3 and 1/6 of the latter. However, as stated already by these authors, the importance of the electrical interaction energy in other alloys cannot be evaluated until more is known about the effective charges on their atoms. Remarkably, the exponent in the three cases is close to the value proposed originally by Mott and Nabarro [4].

References

1. P. HAASEN, "Physical Metallurgy", edited by R. W. Cahn (North Holland, Amsterdam, 1965) p. 821.
2. W. R. HIBBARD, *Trans. AIMME* **1** (1958) 212.
3. J. O. LINDE and S. EDWARDSON, *Ark. f. Fysik* **8** (1954) 511.
4. N. F. MOTT and F. R. N. NABARRO, "Conference on Strength of Solids" (Phys. Soc, London, 1948) p. 1.
5. N. F. MOTT, "Imperfections in Nearly Perfect Crystals" (Wiley, New York, 1952) p. 173.
6. R. L. FLEISCHER and W. R. HIBBARD, "The Relation between Structure and Mechancial Properties of Metals" (Her Majesty's Stationery Office, London, 1963) p. 261.
7. R. L. FLEISCHER, *Acta Metallurgica* **9** (1961) 996.

8. *Idem, ibid* **11** (1963) 203.
9. B. HARRIS, *Phys. Stat. Sol.* **18** (1966) 715.
10. M. M. HUTCHISON and R. W. K. HONEYCOMBE, *Met. Sci. J.* **1** (1967) 70.
11. I. GOEBEL, *Z. Metallk.* **14** (1922) 357; 388; 425; 449.
12. J. E. DORN, P. PIETROWSKY, and T. E. TIETZ, *Trans. AIMME* **188** (1950) 933.
13. D. HARDIE and R. N. PARKINS, *Journal Inst. Metals* **85** (1956) 449.
14. R. L. FLEISCHER, *Acta Metallurgica* **9** (1961) 184.
15. F. WEINBERG, *Can. J. Phys.* **45(2)** (1967) 1189.
16. A. SEEGER, J. DIEHL, S. MADER, and H. REBSTOCK, *Phil. Mag.* **2** (1957) 323.
17. P. FELTHAM and J. D. MEAKIN, *Acta Metallurgica* **5** (1957) 555.
18. G. F. BOLLING, L. E. HAYS, and H. W. WIEDERSICH, *ibid* **10** (1962) 185.
19. P. W. NEURATH and J. S. KOEHLER, *J. Appl. Phys.* **22** (1951) 621.
20. J. VAN DER PLANKEN, M. CRETON, and A. DERUYTTERE, to be published.
21. W. HOFMANN, "Blei und Bleilegierungen" (Springer, Berlin, 1962) p. 96.
22. J. DIEHL, *Z. Metallk.* **47** (1956) 331; 412.
23. M. L. SHEPARD and J. F. SMITH, *Acta Metallurgica* **15** (1967) 357.
24. Y. C. TANG and L. PAULING, *Acta Cryst.* **5** (1952) 39.
25. C. TYZACK and G. V. RAYNOR, *ibid* **7** (1954) 505.
26. H. W. KING, *J. Materials Sci.* **1** (1966) 79.
27. E. TEATUM, K. A. GSCHNEIDNER, and J. WABER, LA-2345, June (1960).
28. J. WABER, K. A. GSCHNEIDNER, A. C. LARSON, and M. Y. PRINCE, *Trans AIMME* **227** (1963) 717.
29. J. R. WILSON, *Metall. Rev.* **10** (1965) nr. 40.
30. A. H. COTTRELL, S. C. HUNTER, and F. R. N. NABARRO, *Phil. Mag.* **44** (1953) 1064.